Computer Assisted Mechanics and Engineering Sciences, 14: 13–23, 2007.

An improved version of artificial boundary node approach

Bahattin Kanber
University of Gaziantep, Mechanical Engineering Department, 27310, Gaziantep, Turkey

(Received August 20, 2004)

This paper proposes an improvement of the artificial boundary node approach using the least square method. The original artificial boundary node approach requires the selection of an offset by the user. The success of the original method depends on the correct choice of the offset. However, the improved version uses a least square line and the solution does not depend on a single offset. The solution is carried on using at least two different offsets and final solution is obtained by replacing the offset as zero in the least square equation. The improved version supplies good accuracy and stability in the boundary element solution. Three different case studies are solved to validate proposed method in 2-D elasticity. All results are compared with each others, conventional BEM, FEM, ANSYS and analytical results whenever possible.

Keywords: Artificial boundary node, boundary element method, least square method, singular integrals

1. Introduction

The boundary integral equation is a statement of the exact solution to the given problem. Therefore, the errors are due primarily to discretization and numerical integration. Accurate and stable solutions can only be obtained if the integrations are sufficiently accurate. The kernel of the integration becomes infinite when the field variable and source point coincide [1]. Some special treatments are required for the solution of these types of singularities. Aliabadi *et al.* [2] developed a technique based on series expansion of the kernel for the treatment of singularities in three dimensional problems. A transformation of variable technique has been proposed by Telles [10] for the integration of singular integrals in two dimensions. Smith [9] presented a direct Gauss quadrature formula for logarithmic singularities in two-dimensional isoparametric elements.

Singular integrals in the boundary element method can also be eliminated by locating the source points on an artificial boundary. The name of this approach is called as artificial boundary or regular boundary element [3]. If the source point is kept in original position at the boundary until source point coinciding with field point, the method is called as artificial boundary node [5–7].

In the artificial boundary node approach, an offset must be used to carry the source point to the outside of the boundary. Because of disturbing the original position of the source points, the solutions always include some amount of errors. A series of offsets can be used instead of using a single offset to reduce the amount of error and to obtain a solution when offset is equal to zero. In this work, a method is proposed for this purpose using the least square method.

2. Boundary integral equations with singularity

A typical boundary integral equation (BIE) can be expressed for elasticity as follows [3],

$$\begin{aligned} c_i u_i + \oint_\Gamma F_{11} u \, \mathrm{d}s + \oint_\Gamma F_{21} v \, \mathrm{d}s - \oint_\Gamma G_{11} T_x \, \mathrm{d}s - \oint_\Gamma G_{21} T_y \, \mathrm{d}s = U(x_i, y_i), \\ c_i v_i + \oint_\Gamma F_{12} u \, \mathrm{d}s + \oint_\Gamma F_{22} v \, \mathrm{d}s - \oint_\Gamma G_{12} T_x \, \mathrm{d}s - \oint_\Gamma G_{22} T_y \, \mathrm{d}s = V(x_i, y_i), \end{aligned} \tag{1}$$

where u_i and v_i are the displacements at the source points, u and v are displacements, and T_x and T_y are tractions on the boundary (Γ), and c_i terms can be written as follows,

$c_i = 1$, for (x_i, y_i) inside the domain (Ω)

$c_i = 0$, for (x_i, y_i) outside Ω, and

$c_i = \frac{\alpha_i}{2\pi}$, for (x_i, y_i) on the boundary (Γ) of the domain (Ω), and α_i is the boundary angle at (x_i, y_i).

$U(x_i, y_i)$ and $V(x_i, y_i)$ include the domain force integrals inside the domain, i.e.,

$$U(x_i, y_i) = \iint_{\Omega} [XG_{11} + YG_{21}]\,\mathrm{d}x\mathrm{d}y,$$
$$V(x_i, y_i) = \iint_{\Omega} [XG_{12} + YG_{22}]\,\mathrm{d}x\mathrm{d}y,$$

where X and Y are the body forces inside the domain (Ω). F is fundamental traction and G is fundamental displacement; i.e.,

$$F_{\alpha\beta} = -\frac{1}{4\pi(1-p)}\frac{1}{r}\left[\frac{\partial r}{\partial n}\left((1-2p)\delta_{ij} + \frac{\partial r}{\partial x_\alpha}\frac{\partial r}{\partial x_\beta}\right) - (1-2p)\frac{\partial r}{\partial x_\alpha}l_\beta\frac{\partial r}{\partial x_\beta}l_\alpha\right], \tag{2}$$

$$G_{\alpha\beta} = \frac{1}{8\pi\mu(1-p)}\left[(3-4p)\ln\left(\frac{1}{r}\right)\delta_{\alpha\beta} + \frac{\partial r}{\partial x_\alpha}\frac{\partial r}{\partial x_\beta}\right], \tag{3}$$

where l_α and l_β are directional cosines and δ is Kronecker delta. μ is the modulus of rigidity and p is as follows,

$p = \nu$ for plane strain problems and

$p = \frac{1}{1+\nu}$ for plane stress problems;

ν is the Poison's ratio. G and F contain singular terms as $-\ln r$ and $\frac{1}{r}$. When the source point and field point coincide with each others, r becomes zero and $-\ln r$ and $\frac{1}{r}$ become indefinite (Fig. 1). The derivation and the application of the treatment of these type of singular integrals have been given by a number of researchers [2, 4, 8–10].

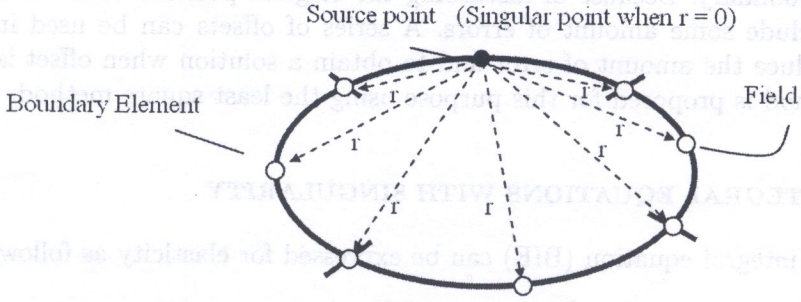

Fig. 1. Conventional boundary element source point

In order to solve the boundary integral equation (1) numerically, the boundary are discretized into a series of elements over which displacements and tractions are written in terms of their values at a series of nodal points. The discretized form of Eq. (1) without any domain load ($X = 0, Y = 0$) can be written as follows,

$$\begin{aligned} c_i u_i + \sum_{e=1}^{n} \left[\oint_{\Gamma_e} (F_{11}\,\mathrm{d}s) u_e + \oint_{\Gamma_e} (F_{21}\,\mathrm{d}s) v_e - \oint_{\Gamma_e} (G_{11}\,\mathrm{d}s)(T_x)_e - \oint_{\Gamma_e} (G_{21}\,\mathrm{d}s)(T_y)_e \right] = 0, \\ c_i v_i + \sum_{e=1}^{n} \left[\oint_{\Gamma_e} (F_{12}\,\mathrm{d}s) u_e + \oint_{\Gamma_e} (F_{22}\,\mathrm{d}s) v_e - \oint_{\Gamma_e} (G_{12}\,\mathrm{d}s)(T_x)_e - \oint_{\Gamma_e} (G_{22}\,\mathrm{d}s)(T_y)_e \right] = 0, \end{aligned} \tag{4}$$

where n is the number of elements in the model.

The type of the boundary element must be decided at this stage. After calculating elemental constants, the boundary conditions can be applied and the solution can be carried out by using ordinary Gauss elimination approach to find unknown displacements and tractions. The stress components at the boundary points are calculated from computed boundary tractions and displacements by simple differentiation using the shape functions. They can be written in the normal and tangential directions at a point in the boundary as follows,

$$\begin{aligned} \sigma_t &= \left(\frac{E}{1-p^2} \right) \varepsilon_t + \left(\frac{p}{1-p} T_n \right), \\ \sigma_n &= T_n, \\ \sigma_{nt} &= T_t, \end{aligned}$$

where E is the Young's modulus and ε_t can be found by differentiating the computed displacement. The relationships between normal and tangential components and x- and y-components can be obtained by using the directional cosines of the boundary point.

3. Artificial boundary node approach

The artificial boundary node approach is another technique to avoid from singularity [5–7] (Fig. 2). In this technique, source points stay at the original boundary until a source point coincides with a field point (1). When a source point and field point coincide, the source point is taken to the outside of the boundary. Therefore, all boundary integrals in terms of such source points become non-singular, and the c_i coefficients in BIEs have zero values. In this case, the first term disappears

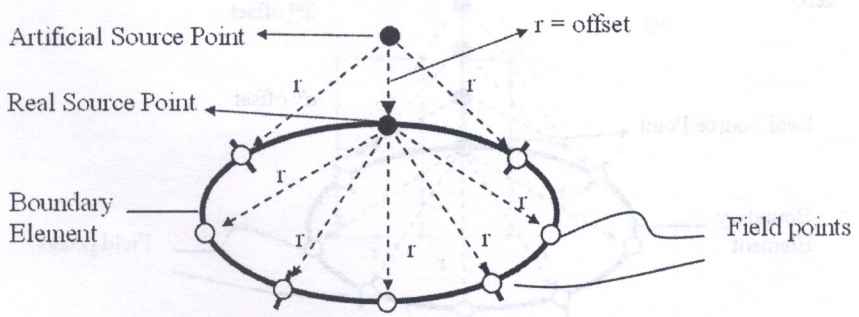

Fig. 2. Artificial and real boundary source points

due to $c_i = 0$ at the outside of the domain in Eq. (1). Then the singularities of BIE vanish as seen in the following equation,

$$\begin{aligned} \oint_\Gamma F_{11} u \, ds + \oint_\Gamma F_{21} v \, ds - \oint_\Gamma G_{11} T_x \, ds - \oint_\Gamma G_{21} T_y \, ds = U(x_i, y_i), \\ \oint_\Gamma F_{12} u \, ds + \oint_\Gamma F_{22} v \, ds - \oint_\Gamma G_{12} T_x \, ds - \oint_\Gamma G_{22} T_y \, ds = V(x_i, y_i). \end{aligned} \tag{5}$$

4. Improved Artificial Boundary Node Approach

In the artificial boundary node approach, the singularities are avoided using offsets at source points as mentioned. All results which are found by this method include some amount of errors because of these offsets. The amounts of these errors are proportional with the amount of offsets used in solution. When offsets approach to zero, the results also approach to the accurate results. However, they never reach to the accurate results in some cases. When very small offsets are used, the stress and displacements becomes nearly constant because of the precision limits of calculations. The amount of errors can be reduced by increasing the number elements in the discretization as shown in [5–7].

The artificial boundary node approach can be improved considering the effects of offsets in the solutions. At any node in the boundary, different solutions can be obtained while a source point is approaching to original location. Figure 3 shows the locations of a source point when the offset is approaching zero. For larger offset values, the displacements and stresses diverges from exact values and for small offsets, they become nearly constant. Between divergence limit and constant value limit, the results show a nearly linear distribution. The limits of linear distribution interval may be determined by following offset values: For mid-nodes in an element, $Max.Off$ = *element length*/10 and $Min.Off$ = *element length*/100. For edge-nodes in an element, $Max.Off$ = (*length of preceding element* + *length of following element*)/10 and $Min.Off$ = (*length of preceding element* + *length of following element*)/100.

These offsets are used in order to generalize the improved method and may be changed. But they give acceptable results for many examples. So an extrapolation can be done to predict the corrected values for stress and displacement when offset is equal to zero. Least square line can be used for this purpose as follows,

$$Rst = a_0 + a_1 * off\,, \tag{6}$$

$$a_1 = \frac{n \sum (off_i \, Rst_i) - \sum off_i \sum Rst_i}{n \sum off_i^2 - \left(\sum off_i\right)^2}, \tag{7}$$

$$a_0 = \overline{Rst} - a_1 \, \overline{off}\,, \tag{8}$$

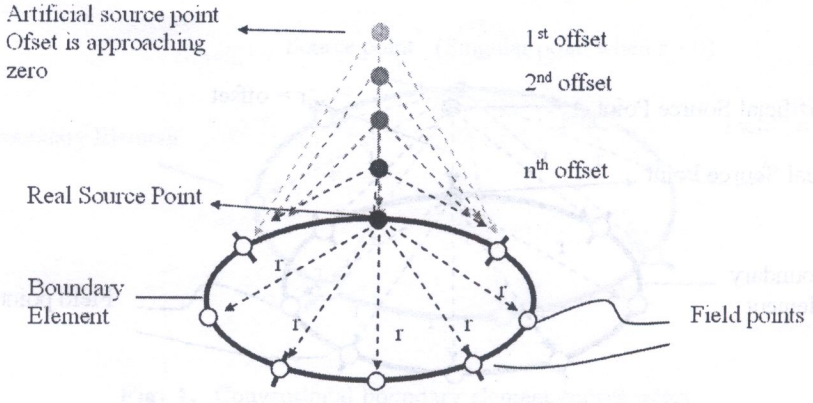

Fig. 3. Artificial source point while offset is approaching zero

where n is the total number of different offsets used in the solution, off_i is the value of offset for i-th solution, Rst is any displacement or stress components obtained by artificial node approach, $\overline{Rst}$ is the arithmetic mean of Rst_i and $\overline{off}$ is the arithmetic mean of off_i.

After the least square line is constructed, the corrected value of any displacement or stress component can be obtained by replacing offset value as zero (i.e. $off = 0$). Other unknown quantities such as tractions and strains can be found using corrected values.

5. Case studies and discussion

Three different two-dimensional problems are analysed using improved method. Their results are compared with conventional BEM, FEM, ANSYS and analytical solutions. They are discretized into uniform boundary and finite elements with equal element lengths. Consequently, equal offsets are used for different boundary elements in the artificial boundary node approach. The following abbreviations are used in all examples.

ImpABN is the improved artificial boundary node approach. Three different offsets are used ($n = 3$).

ABNoff = le/100 shows artificial boundary node approach with offset of $le/100$ (le = length of boundary element).

ABNoff = le/50 is used for artificial boundary node approach with offset of $le/50$.

ABNoff = le/10 denotes artificial boundary node approach with offset of $le/10$.

ConvBEM is the conventional boundary element method.

5.1. Thin Plate

In this example, a thin plate is clamped at one end and loaded with uniform horizontal traction at the other end as shown in Fig. 4a. It is considered as plane stress problem. Aluminium is used as the material of the plate ($E = 70\,\text{GPa}$, $\nu = 0.27$). In the boundary and finite element discretizations,

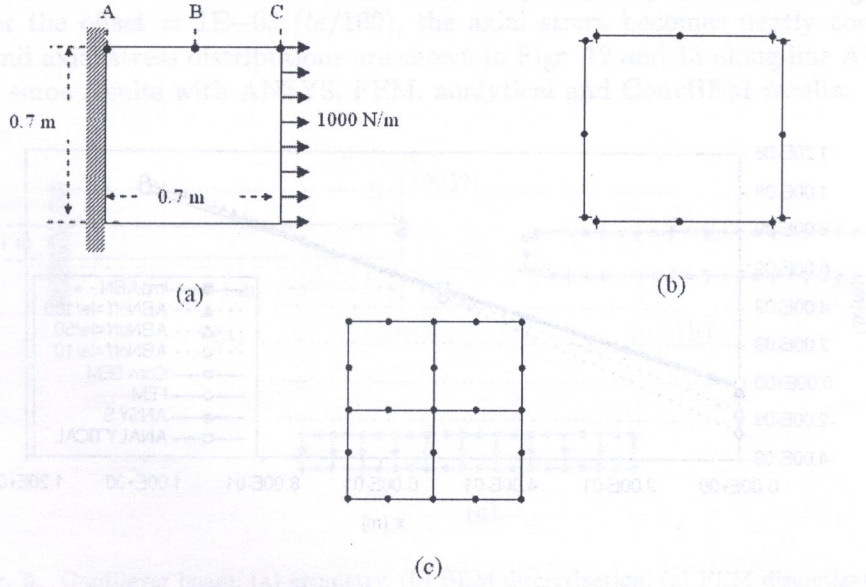

Fig. 4. Thin plate: (a) geometry, (b) BEM discretization, (c) FEM discretization

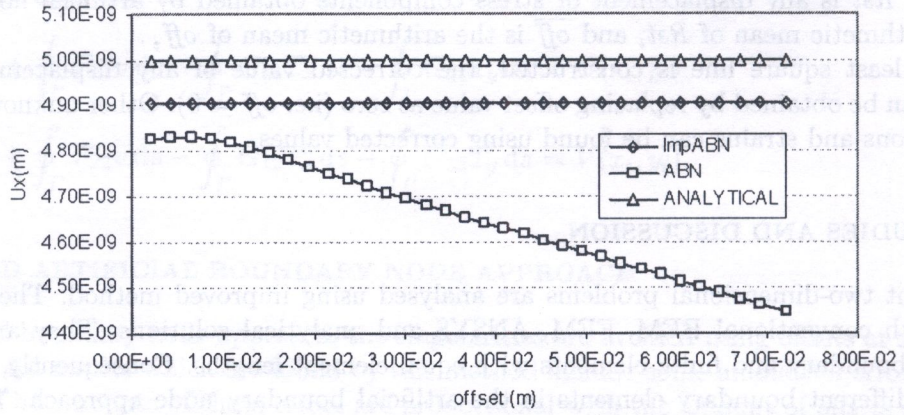

Fig. 5. Axial displacement variation at point B on the plate while offset is approaching zero

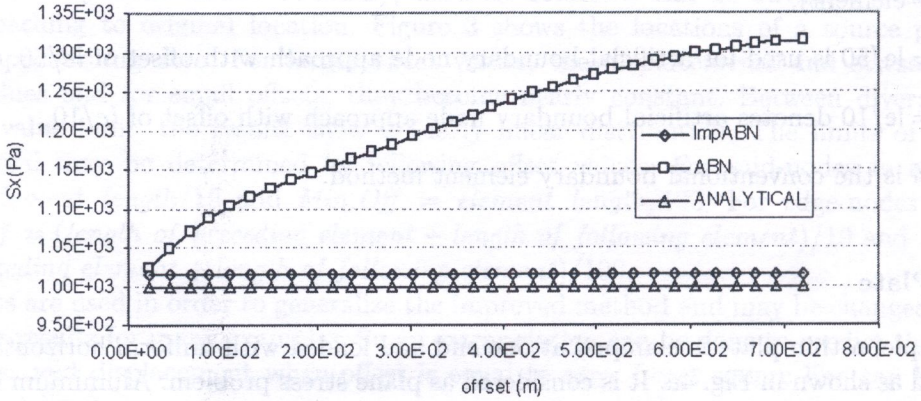

Fig. 6. Axial stress variation at point B on the plate while offset is approaching zero

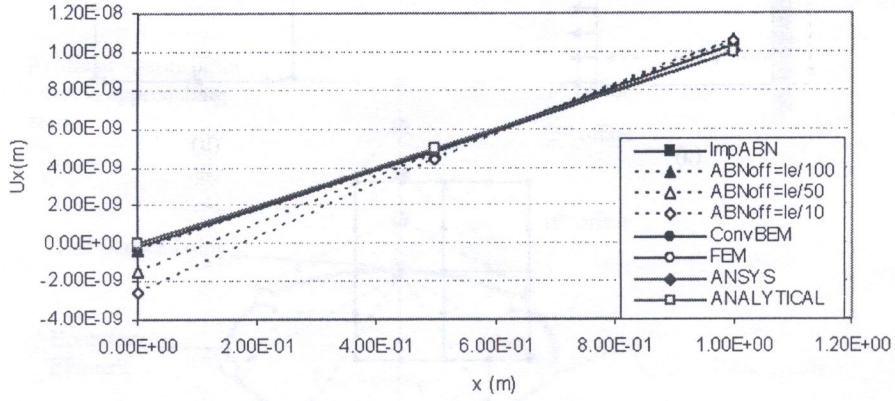

Fig. 7. Axial displacement distribution along ABC line on the plate

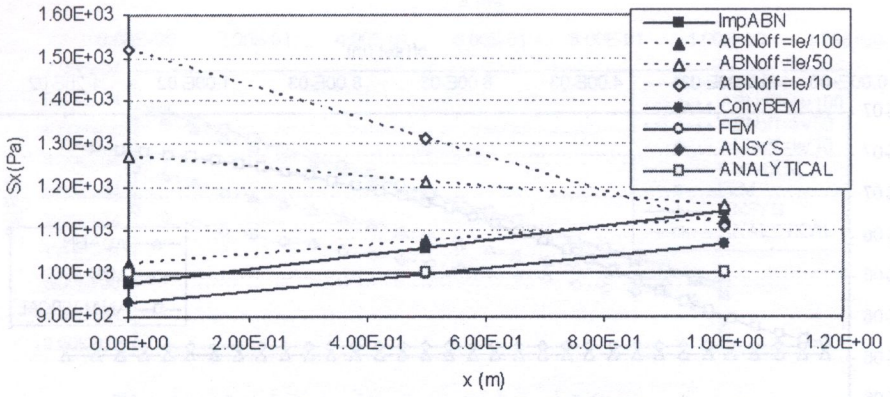

Fig. 8. Axial stress distribution along ABC line on the plate

4 quadratic elements are used (Figs. 4b,c). Figure 5 shows the axial displacement variation against different offsets at point B on the plate. As offset is approaching to zero, the axial displacement is approaching to the analytical solution. However, it can't reach. After the offset value of 0.007 (i.e. $le/100$), the axial displacement becomes nearly constant. The axial stress, however, reaches the analytical solution for small offsets (Fig. 6). The axial displacement distribution is shown in Fig. 7 along line ABC on the plate. The results of ABN get better as the offsets decreases ($le/10$, $le/50$, $le/100$). ImpABN gives same results with ANSYS, analytical, FEM and ConvBEM results. Similar improvements can be seen in Fig. 8 for axial stress distribution along the same line.

5.2. Cantilever beam

Cantilever beam problem is used as the second example. A vertical load is applied at the end of the beam (Fig. 9a). The beam is assumed to be made of a steel alloy ($E = 200\,\text{GPa}$, $\nu = 0.3$) and solved as plane strain problem. In the boundary element discretization, 22 quadratic elements are used (Fig. 9b). The beam is discretized into 10 quadratic finite elements (Fig. 9c).

Vertical displacement reaches analytical solution as the offset approaches zero at point B for the beam (Fig. 10). Axial stress, on the other hand, can not reach analytical solution at the same point (Fig. 11). After the offset = 1E−03 ($le/100$), the axial stress becomes nearly constant. Vertical displacement and axial stress distributions are shown in Figs. 12 and 13 along line AB on the beam. ImpABN gives same results with ANSYS, FEM, analytical and ConvBEM results.

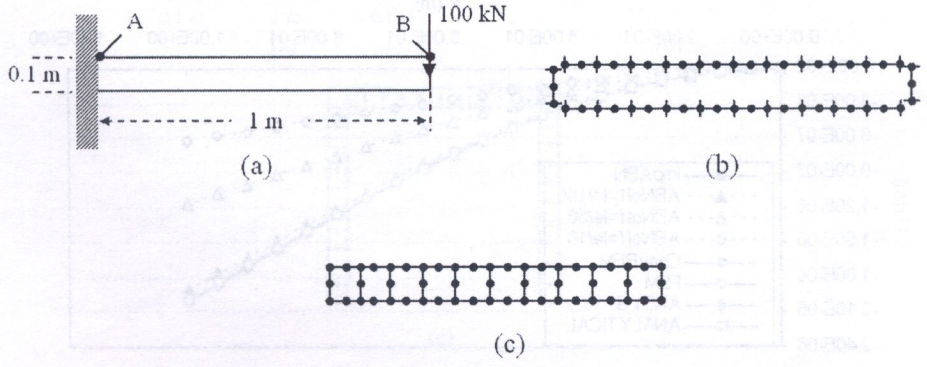

Fig. 9. Cantilever beam: (a) geometry, (b) BEM discretization, (c) FEM discretization

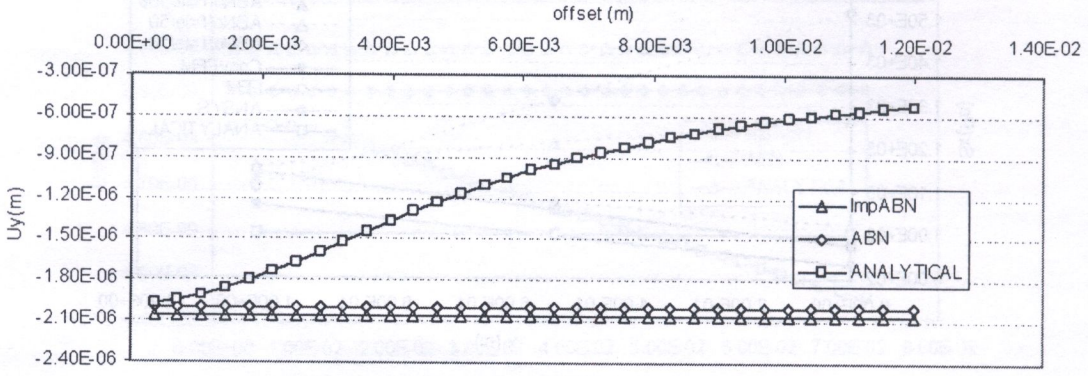

Fig. 10. Vertical displacement variation at point B on the beam while offset is approaching zero

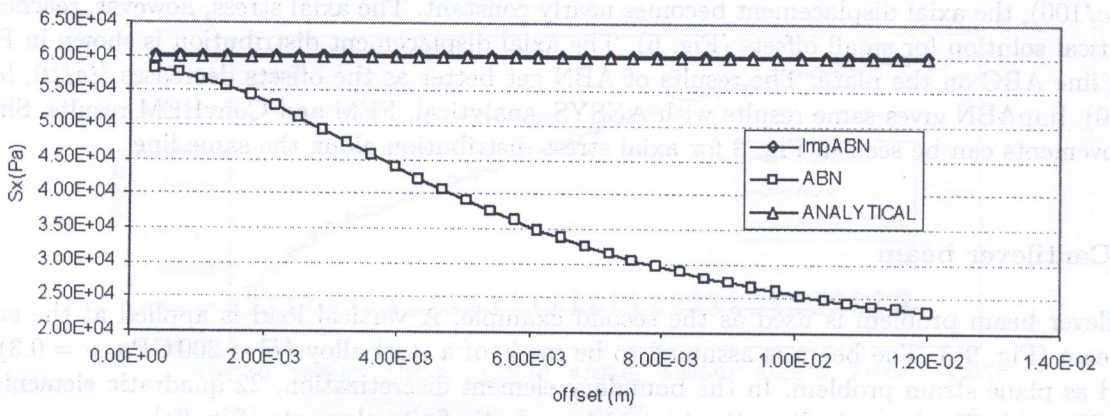

Fig. 11. Axial stress variation at point A on the beam while offset is approaching zero

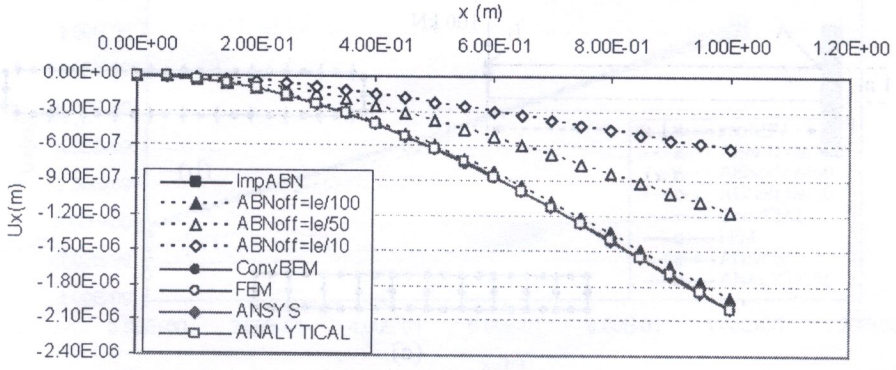

Fig. 12. Vertical displacement distribution along AB line on the beam

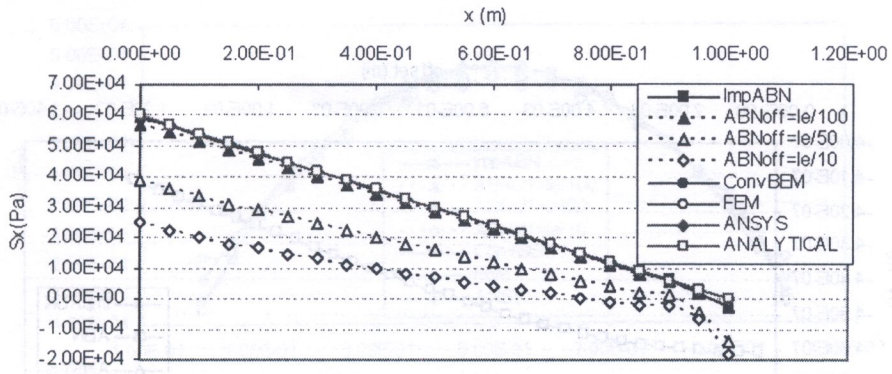

Fig. 13. Axial stress distribution along AB line on the beam

5.3. Portal frame

The geometry and boundary conditions of frame is shown in Fig. 14a. The material is again steel ($E = 200\,\text{GPa}$, $\nu = 0.3$). The frame is considered under plane strain conditions and discretized into 66 quadratic boundary elements (Fig. 14b). In the finite element model, however, 32 quadratic elements are used as shown in Fig. 14c. The vertical displacements and axial stresses of ABN can not reach ANSYS results as offset approaches zero at point B on the frame. After the offset = 1E−03 ($le/100$), they become constant (Figs. 15 and 16). This constant distribution is corrected by ImpABN as shown. ImpABN gives same results with ConvBEM in vertical displacement and axial stress distributions along line ABC on the frame as shown in Figs. 17 and 18.

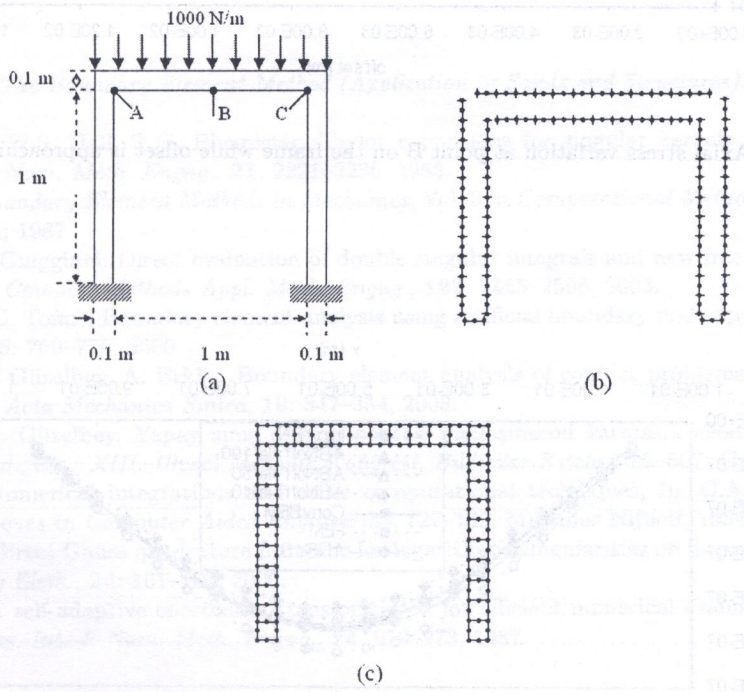

Fig. 14. Portal frame: (a) geometry, (b) BEM discretization, (c) FEM discretization

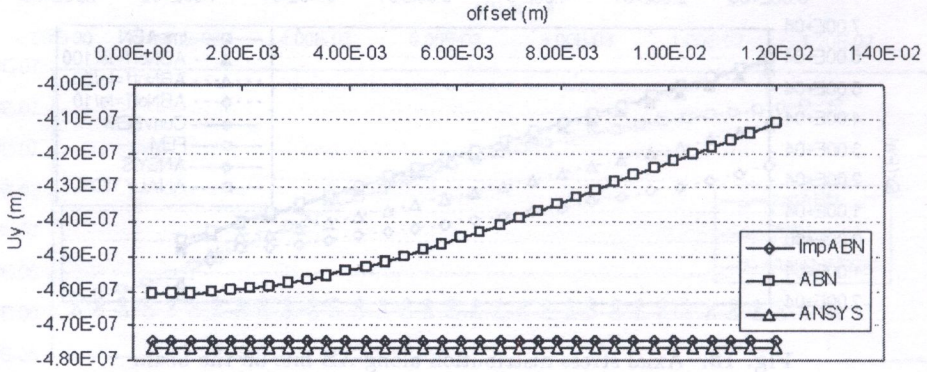

Fig. 15. Vertical displacement variation at point B on the frame while offset is approaching zero

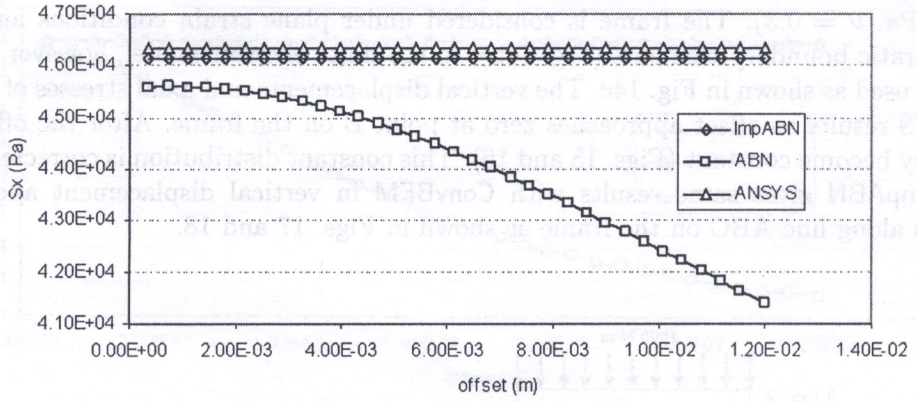

Fig. 16. Axial stress variation at point B on the frame while offset is approaching zero

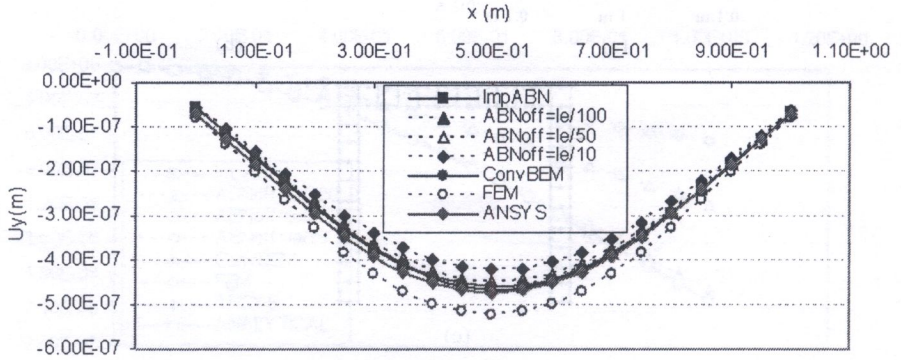

Fig. 17. Vertical displacement distribution along ABC line on the frame

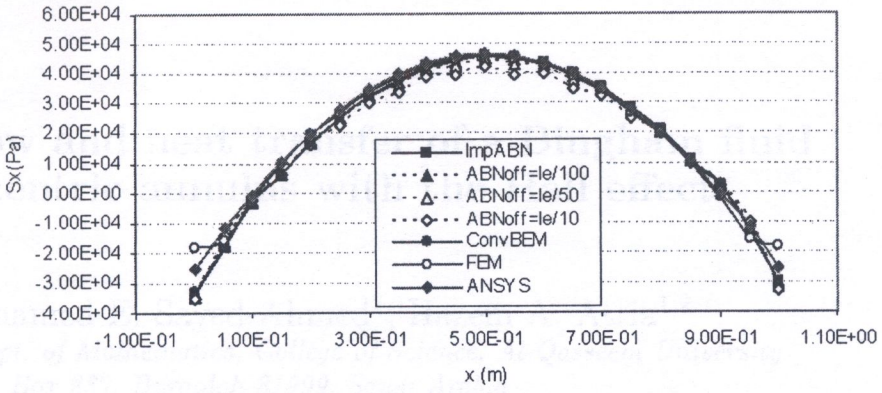

Fig. 18. Axial stress distribution along ABC line on the frame

6. Conclusion

The artificial boundary node approach has been improved using the least square method. It was shown that the accuracy and stability of the boundary element solutions can be increased using the improved version of artificial boundary node approach. The accuracy of the improved method depends on the total number of different offsets, n. It was selected as 3 in this work. High number of offsets increases the accuracy of the method. But it causes more solution time.

One of the problems in the artificial boundary node approach is the selection of the right offset. The improved artificial boundary node approach does not have such a problem. Due to the least square line, there is no need to investigate for the right offset. It also supplies a solution without singularity when the offset becomes zero.

References

[1] M.H. Aliabadi. *The Boundary Element Method (Application in Solids and Structures)*, Vol. 2. Wiley, New York, USA, 2002.

[2] M.H. Aliabadi, W.S. Hall, T.G. Phemister. Taylor expansions for singular kernels in the boundary element method. *Int. J. Num. Meth. Engng.*, **21**: 2221–2236, 1985.

[3] D.E. Beskos. *Boundary Element Methods in Mechanics*, Vol. 3 in *Computational Methods in Mechanics*. Elsevier, New York, USA, 1987.

[4] M. Bonnet, M. Guiggiani. Direct evaluation of double singular integrals and new free terms in 2D (symmetric) Galerkin BEM. *Comput. Methods Appl. Mech. Engng.*, **192**: 2565–2596, 2003.

[5] I.H. Guzelbey, G. Tonuc. Boundary element analysis using artificial boundary node approach. *Commun. Numer. Meth. Engng*, **16**: 769–776, 2000.

[6] B. Kanber, I.H. Güzelbey, A. Erklig. Boundary element analysis of contact problems using artificial boundary node approach. *Acta Mechanica Sinica*, **19**: 347–354, 2003.

[7] B. Kanber, İ.H. Güzelbey. Yapay sınır düğüm noktası yaklaşımının karmaşık geometrilere uygulanması. In: H. Demiray *et al.*, eds., *XIII. Ulusal Mekanik Kongresi, Bildiriler Kitabı*, 499–507. Gaziantep, 2003.

[8] H.L.G. Pina. Numerical integrations and other computational techniques, In: C.A. Brebbia, ed., *Boundary Element Techniques in Computer Aided Engineering*, 127–139. Martinus Nijhoff, 1984.

[9] R.N.L. Smith. Direct Gauss quadrature formulae for logarithmic singularities on isoparametric elements. *Engng. Anal. Boundary Elem.*, **24**: 161–167, 2000.

[10] J.C.F. Telles. A self-adaptive coordinate transformation for efficient numerical evaluation of general boundary integral elements. *Int. J. Num. Meth. Engng.*, **24**: 959–973, 1987.